Original Research Article **Medicinal Biochemistry**

International Journal of Pharma and Bio Sciences

ISSN 0975-6299

CURCUMIN ANALOGUE 1,5-BIS (4-HYDROXY-3-METHOXYPHENYL)-1,4-PENTADIENE-3-ONE ALTERS PROTEIN EXPRESSION PATTERNS IN HPV16-INFECTED CERVICAL CANCER CELLS

JIN HUNG CHEW[1], FELICIA PAULRAJ[1], FARIDAH ABAS[2,3], NORDIN H. LAJIS[2], IEKHSAN OTHMAN[1], RAKESH NAIDU[*1]

[1] Jeffrey cheah school of medicine & health sciences, monash university malaysia, jalan lagoon selatan, bandar sunway 47500, selangor, malaysia
[2]Laboratory of natural products, faculty of science, universiti putra malaysia, upm serdang 43400, selangor, malaysia
[3]Department of food science, faculty of food science and technology, universiti putra malaysia, upm serdang 43400, selangor, malaysia.

ABSTRACT

Curcumin analogue 1,5-bis (4-hydroxy-3-methoxyphenyl)-1,4-pentadiene-3-one (MS13) has been shown to exhibit significant cytotoxic and anti-proliferative activity. In the present study, protein expression profile of MS13-treated HPV-16 positive CaSki human cervical cancer cells was determined using two-dimensional gel electrophoresis and identified differentially expressed proteins by mass spectrometry. Eighty two up-regulated and 11 down-regulated proteins were identified in response to 48 h of 3.5µM MS13 treatment. Functional analysis revealed that the highly up-regulated proteins were associated with metabolic process (CAPNS1, PDXK, MTHFD1, ACADVL and NPM1), cell communication (ARHGDIB), cell cycle and apoptosis (LMNA), transcriptional regulation (SRSF1 and SRSF7) and translational regulation (DDX47) whereas highly down-regulated proteins were associated with metabolic process (ALDOA, ATP5B and ANXA5), protein folding (HSP90B1 and HSP90AB2P), structural molecule activity (ACTN4) and transcriptional regulation (HNRNPL). These findings revealed that MS13 may exhibit its anticancer properties on cervical cancer cells through regulation of these proteins.

KEYWORDS: *diarylpentanoid, cervical cancer, proteomic profiling, mass spectrometry, curcumin analogue*

RAKESH NAIDU*

Jeffrey cheah school of medicine & health sciences, monash university malaysia, jalan lagoon selatan, bandar sunway 47500, selangor, malaysia

Received on: 02-06-2017
Revised and Accepted on: 03-10-2017
DOI: http://dx.doi.org/10.22376/ijpbs.2017.8.4.b391-403

INTRODUCTION

Cervical cancer remains one of the major causes of mortality among women worldwide despite the effort and progress that has been made in the prevention, diagnosis and treatment of the disease.[1] Over 99% of cervical cancers were found to be associated with persistent human papillomavirus (HPV) infection.[2] HPV-16 is the most oncogenic strain, followed by HPV-18.[3,4] Both strains account for approximately 70% of all cervical cancers.[5] Curcumin (diferuloyl methane), a natural compound extracted from turmeric (*Curcuma longa*), has been shown to exhibit anticancer properties through the modulation of various molecular pathways and induces biological effects such as anti-inflammatory, anti-tumorigenic, anti-mutagenic, anti-metastatic and anti-angiogenic properties *in vitro* and *in vivo.*[6,7] Curcumin has shown apoptotic and anti-proliferative activity in cervical cancer cells through downregulation of transcription factor NF-κB and downstream gene products including pro-inflammatory cytokine COX-2[8] and apoptosis regulator Bcl-2.[9] Curcumin also induces cell cycle arrest by suppressing the expression of cyclin D1, regulator of cyclin-dependent kinase (CDKs) which is required for cell cycle progression.[9,10] Curcumin's diverse array of molecular targets affords it great potential as a chemotherapeutic agent but its clinical applicability is limited by its low systemic bioavailability.[11] Structural modification of curcumin represents a strategy to improve its stability and pharmacokinetic properties. Recently, a series of new curcumin analogues with 5-carbon chain between aryl rings, known as diarylpentanoids has shown to display greater growth inhibitory effect and higher effectiveness in inducing apoptosis in human cervical[12], pancreatic[13], breast and prostate cancer cells[14] in comparison to curcumin. Although several investigators have demonstrated anticancer activities of diarylpentanoids on various cancers, studies investigating the anticancer effect on cervical cancer are limited. In order to understand the anticancer mechanism of diarylpentanoid, we have analysed the protein expression profiles of cervical cancer cells treated with diarylpentanoid MS13 using two-dimensional gel electrophoresis (2DE). Significant differentially expressed protein (DEP) spots ($p<0.05$) were selected for protein identification using nanoflow liquid choromatography electrospray-ionisation coupled with mass spectrometry/mass spectrometry (LC-MS/MS) and bioinformatics. The biological functions of these DEPs were studied to provide a better understanding of the anticancer mechanism of MS13.

MATERIALS AND METHODS

Chemicals and reagents

RPMI-1640, Fetal Bovine Serum and penicillin (100U/mL)/streptomycin (100µg/mL) were purchased from Gibco®, USA. DMSO, Triton® X-100, bromophenol blue, iodoacetamide, formaldehyde and potassium ferricynade were purchased from Sigma-Aldrich, USA; urea, thiourea, glycerol, SDS, Tris, acetic acid, sodium thiosulfate, silver nitrate, sodium carbonate, hydrochloric acid and ammonium bicarbonate from Merck, USA; CHAPS, DTT, IPG buffer (pH 3-10) and 2D Quan Kit from GE Healthcare, UK; protease inhibitor, RNAse A and trypsin from Thermo Scientific, USA; acetonitrile from Fisher Scientific, USA; Dnase I from Qiagen, Venlo, Limburg and formic acid from Fluke, USA.

Cell culture and synthesis of diarylpentanoid

HPV-16 positive human cervical cancer cells, CaSki was obtained from American Type Culture Collection (ATCC, USA). CaSki cells were cultured in RPMI-1640 and supplemented with 10% Fetal Bovine Serum and penicillin (100U/mL)/streptomycin (100µg/mL). Cultured cells were grown at 37°C in a humidified atmosphere of 5% CO_2. The diarylpentanoid, 1,5-bis(4-hydroxy-3-methoxyphenyl)-1,4-pentadiene-3-one (MS13) was synthesised as previously described [15].

Treatment with diarylpentanoid

The cells were plated in T75 culture flasks (Nunc, Denmark) in culture media and incubated at 37°C with 5% CO_2 in humidified incubator for 24 h. MS13 was prepared in a stock concentration of 50mM using DMSO and the treatment dose of EC_{50}=3.5µM was obtained by dilution in culture medium. Following 24 h of cell plating, CaSki cells were treated with 0.01% DMSO (negative control) or 3.5µM of MS13 for 48 h. The experiment included negative controls and was performed in triplicate with three biological replicates.

Sample preparation for 2DE

At the end of 48 h incubation period, cells were pelleted, washed with ice-cold PBS and suspended in 200µL of extraction buffer composed of 7M urea, 2M thiourea, 4% CHAPS, 65mM DTT, 1% protease inhibitor and 2% IPG buffer (pH 3-10). Suspension was vortexed on ice at 2500 rpm for 2 mins and frozen on dry ice for 10 mins. The second cycle of freeze-thaw was performed with 5 mins of vortexing. The samples were vortexed on ice at 2500 rpm for 15 mins. DNAse I and RNAse A at final concentrations of 20 units/mL and 0.25 mg/mL respectively were added to degrade nucleic acid and incubated on ice for 45 mins. The lysate was centrifuged at 13,000 x *g* at 4°C for 1 h. The protein concentration was determined using 2D Quan Kit.

2-Dimensional gel electrophoresis (2DE)

Individual sample amount was adjusted by dilution in rehydration buffer (7M urea, 2M thiourea, 2% (w/v) CHAPS, 65mM DTT, 0.2% Triton® X-100, 0.002% bromophenol blue, 0.5% (v/v) IPG buffer pH 3-10) to a final protein concentration of 1.1mg in 300uL and incubated at room temperature for 30 mins. A total of 1.1mg of protein samples were loaded onto immobilised pH gradient (IPG) strips (13cm, pH 3-10, linear, GE Healthcare) for 16 h passive rehydration at room temperature. Isoelectric focusing (IEF) was performed using Ettan IPGphor3 platform (GE Healthcare) at 20°C following the parameters: 500V for 2 h 20 mins, hold; 1000V for 1 h, gradient; 8000V for 2 h 30 mins, gradient, and 8000V for 30 mins, hold. Isoelectric-focused strips were equilibrated in equilibration buffer (6M urea, 30% (v/v) glycerol, 2% (w/v) SDS, 375mM Tris (pH8.8), 0.002% bromophenol blue, 1% (w/v) DTT for 30 mins, followed by the same buffer containing 2.5% (w/v) iodoacetamide instead of DTT for 30 mins. Second dimensional SDS-PAGE was performed on 12% uniform

SDS-polyacrylamide gels at 90V for 30 mins and then 200V until the dye front reached the bottom of the gels using Hoefer SE600 (GE Healthcare). The experiment was repeated three times to ensure reproducibility.

Protein visualisation and image analysis

The gels were fixed overnight in 50% ethanol and 12% acetic acid, and washed 3 times for 20 mins each in 20% ethanol. Gels were sensitised in 0.02% (w/v) sodium thiosulfate and washed in double distilled water twice for 15 s each. The gels were stained with 0.2% (w/v) silver nitrate and 0.076% formaldehyde for 15 mins, washed twice in double distilled water for 1 min each, then developed in 6% (w/v) sodium carbonate, 0.0004% sodium thiosulfate, 0.05% formaldehyde for 5 mins and stopped in 12% acetic acid. The gel images were captured using ChemiDoc™ XRS Imaging System (Bio-Rad, USA) and Quantity One® software (Bio-Rad). 2DE gel images were analysed by PDQuest software version 8.0.1 (Bio-Rad). The PDQuest software was used to subtract background, normalise and match gels, and to assign identification and calculate intensity to each protein spot. Sensitivity value of 14.9, minimal peak value of 1400 and Gaussian modelling were applied for spot detection. Relative comparison of the intensity abundance between control and treated group was performed using Student's t-test. Protein spots selected for identification met the following criteria: (i) t-test value ($p<0.05$), (ii) at least 1.5-fold change, and (iii) the identification of the spot in 2 out of 3 replicates.

In-gel tryptic digestion

Protein spots were manually excised from the gels. Gel plugs were destained in 30mM potassium ferricynade and 100mM sodium thiosulfate until the brown colour disappeared, then washed for 5-10 mins at least 5 times, until the solution was clear. An aliquot of 0.4µg of trypsin in 1mM hydrochloric acid and 40mM ammonium bicarbonate in 9% acetonitrile was added to digest the gel plugs and incubated overnight at 37^{o}C. Supernatant were collected. The tryptic digested peptides were extracted using 5% formic acid, incubated at 37^{o}C for 15 mins, and the supernatant was pooled. Protein extraction was repeated using 5% formic acid in 50% acetonitrile, and High Performance Liquid Chromatography (HPLC) grade pure acetonitrile. The pooled extracts were dried overnight in a centrifugal evaporator CVE-3100 (Eyela, Japan) at a rotation speed of 1000 rpm at 60^{0}C.

LC-MS/MS and data analysis

The dried peptides were reconstituted with 5µL of 0.1% formic acid in water and loaded into Agilent C18 300A Large Capacity Chip (Agilent Technologies, USA) and equilibrated with 0.1% formic acid in water. Peptides were eluted from the column with the following gradient: 3-50% formic acid in water from 0-30 minutes, 50-95% formic acid in water from 30-32 minutes and maintained at 95% formic acid in water from 32-39 minutes. Q-TOF polarity was set at positive with capillary and fragmentor voltage being set at 2050V and 300V respectively, and 5L/minute of gas flow at 300^{o}C. Protein spectra were analysed in auto MS mode ranging from 110-3000 m/z for MS scan and 50-3000 m/z for MS/MS scan. The data obtained from LC-MS/MS was processed with PEAKS Studio 7.0 (Bioinformatics Solution, Waterloo, Canada). Protein homology of each sample was searched against *Homo sapiens* protein database in National Center for Biotechnology Information (NCBI) (Aug 2013) by comparing the *de novo* sequence tag. Carbamidomethylation was set as fixed modification and maximum mixed cleavages at 3. Parent mass and fragment mass error tolerance were both set at 0.1Da with monoisotopic as precursor mass search type. Search results were filtered based on the following criteria: (i) false discovery rate (FDR) ≤ 1%, (ii) PEAKS score (-10logP) ≥ 40, and (iii) non-hypothetical protein. MS/MS spectra were also searched against cRAP protein database in The Global Proteome Machine (The GPM) (Version 2012.01.01) to eliminate the possible common contaminants.

Protein Functional Classification

Official gene symbols of DEPs were obtained from Ingenuity Pathway Analysis (IPA) and uploaded into Protein Analysis Through Evolutionary Relationships (PANTHER^{TM}) classification system (http://pantherdb.org/) to classify them according to their functions by matching the gene symbols to PANTHER^{TM} GO slim. The unmatched gene symbols were then uploaded to The Database for Annotation, Visualization and Integrated Discovery (DAVID) Bioinformatics Resources 6.7 (https://david.ncifcrf.gov/) for further functional classification. Functional annotation was performed based on biological process and limited to *Homo sapiens*.

RESULTS

Our previous study has demonstrated that a dose of approximately 3.5µM MS13 resulted in 50% reduction in CaSki cell viability at 48 h (EC_{50}).[12] Based on these results, we investigated the protein expression profile and identified DEPs to elucidate the potential anticancer mechanism in human cervical cancer cells. Representative 2DE gel images of control and 3.5µM MS13-treated cells are shown in Figure 1. A total of 16 protein spots demonstrated significant difference ($p<0.05$) over 1.5-fold change in MS13-treated cells compared to control cells. The up- and down-regulated proteins were assessed qualitatively. Amongst these, 12 spots were up-regulated and 4 spots were down-regulated in response to MS13 treatment. Overall, 82 proteins were identified from the 12 up-regulated protein spots whereas 11 proteins were determined from 4 down-regulated spots. Proteins with -10lgP score that met or exceeded the threshold of 40 were presented in Tables 1 and 2. The up-regulated DEPs were categorised into 10 functional groups with metabolic process (21%) accounted for the major proportion, followed by structural molecule activity and cytoskeletal organisation (16%), transport (10%), cell communication (8%), protein folding (7%), redox regulation and detoxification (7%), transcriptional regulation (7%), cell cycle and apoptosis processes (7%), proteolysis (6%) and translational regulation (6%) (Figure 2). The down-regulated proteins were categorised into 7 groups with metabolic process (28%) contributing towards the highest percentage followed by protein folding (18%). Nine percent of the functional groups were respectively composed of proteolysis, cell cycle, structural molecule

activity, immune system process and transcriptional regulation (Figure 3). Approximately 5% of upregulated and 9% of down-regulated proteins were not associated with biological functions and were annotated as 'Unknown'. In the present study we have identified several highly up- and down-regulated proteins with fold-changes ranging from 1.97 to 3.05 and 1.76 to 2.67, respectively. The up-regulated proteins included ARHGDIB that was associated with cell communication, CAPNS1, PDXK, MTHFD1, ACADVL and NPM1 with metabolic process, LMNA with cell cycle and apoptosis, SRSF1 and SRSF7 with transcriptional regulation, and DDX47 with translational regulation. Amongst the highly down-regulated proteins ALDOA, ATP5B and ANXA5 were associated with metabolic process, HSP90AB2P and HSP90B1 with protein folding, ACTN4 with structural molecule activity and HNRNPL with transcriptional regulation.

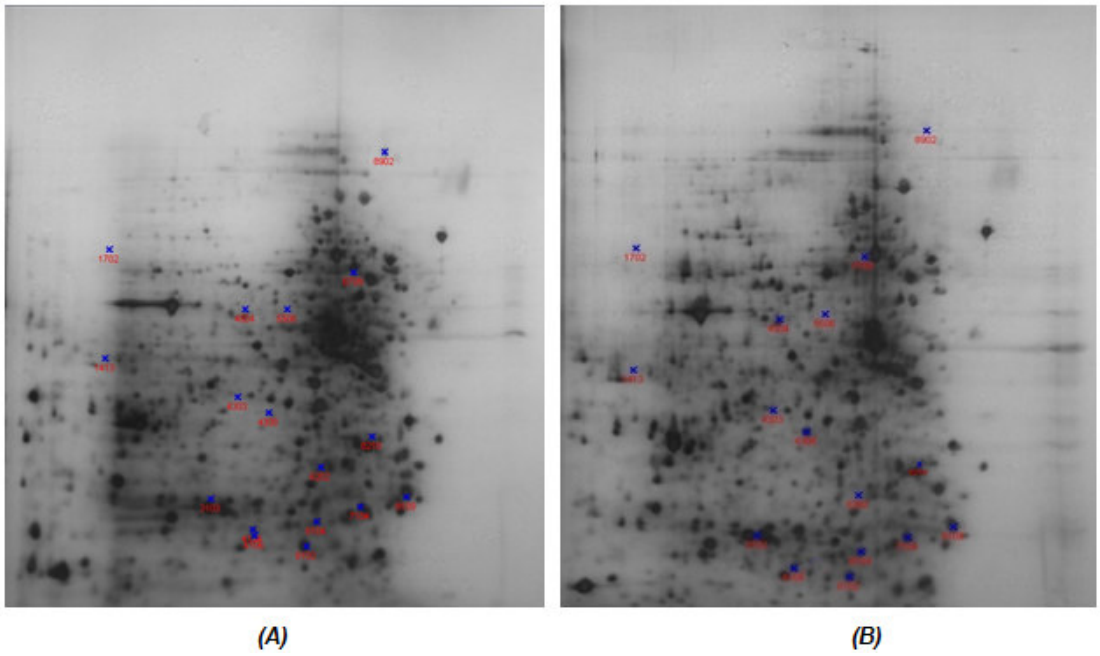

Figure 1
2DE gel analysis of protein expression in (A) untreated as control and (B) 3.5µM MS13-treated CaSki cells.

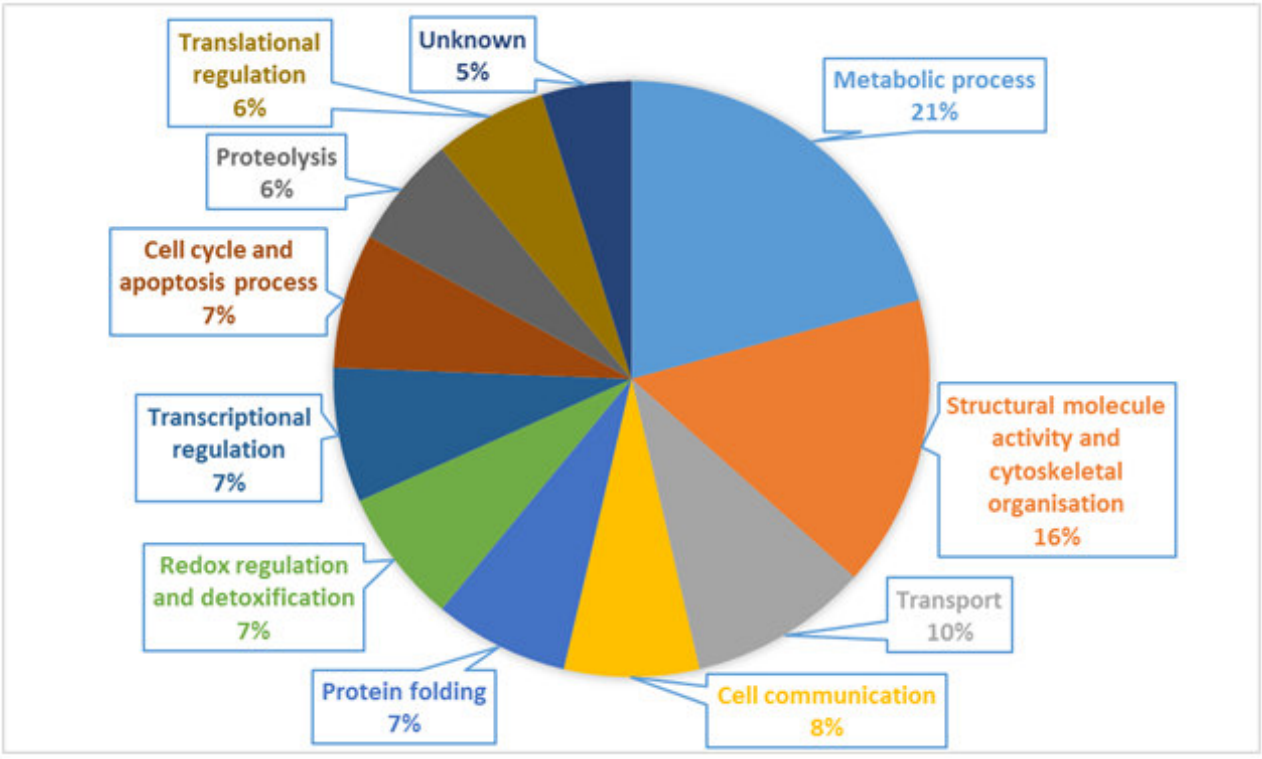

Figure 2
Function classification of up-regulated DEPs based on biological process using PANTHER™ system and DAVID Bioinformatics Resources 6.7.

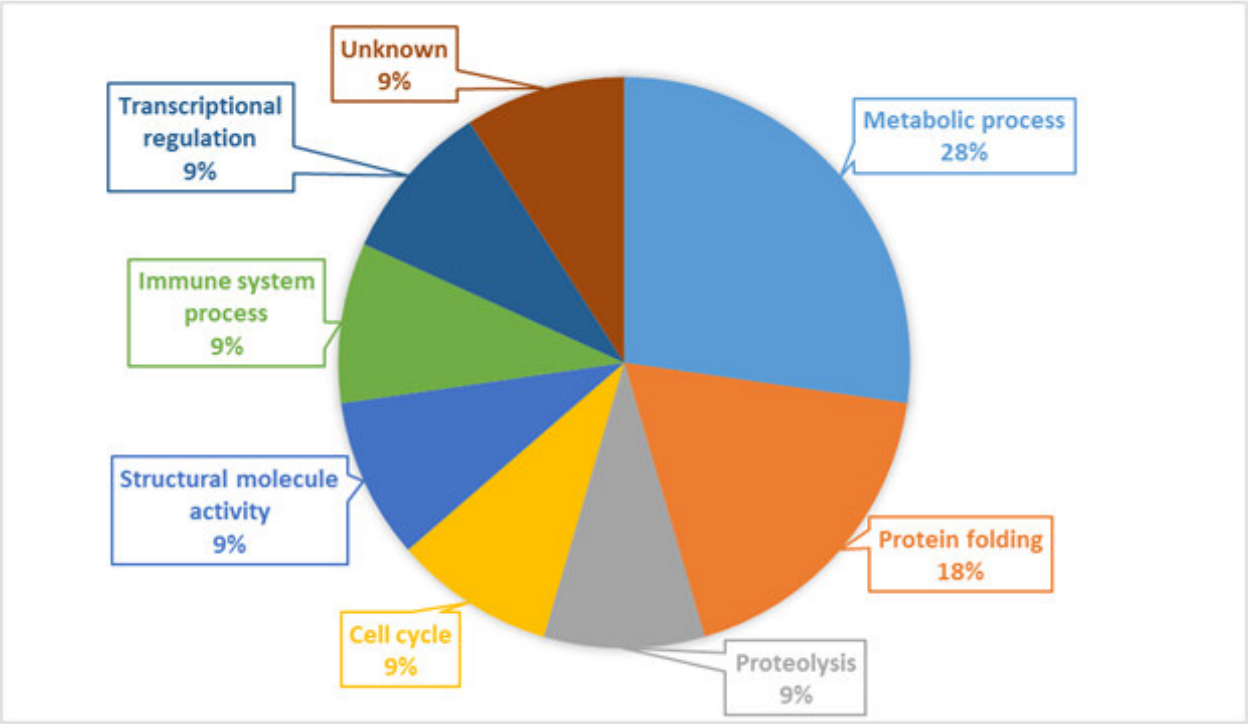

Figure 3
Function classification of down-regulated DEPs based on biological process using PANTHER™ system and DAVID Bioinformatics Resources 6.7.

Table 1
Functional classification of up-regulated proteins in CaSki cells treated with 3.5μM MS13.

SSP no.	Gene symbol	Accession	-10lgP	Coverage (%)	#Peptides	#Unique	Avg. Mass	Log_2 fold change	Protein description
Cell communication									
7104	ARHGDIB	gi|119616745	51.87	21	2	1	20703	3.05	Rho GDP-dissociation inhibitor 2
7601	PRKAR1A	gi|179895	67.83	12	5	5	42982	1.76	cAMP-dependent protein kinase type I-alpha regulatory subunit
3103	SEPT2	gi|15680208	53.56	4	2	2	41477	1.74	Septin-2
8109	SFN	gi|187302	288.17	81	75	2	27776	1.48	14-3-3 protein sigma
8109	YWHAQ	gi|54696890	168.2	57	23	2	27763	1.48	14-3-3 protein theta
8109	YWHAB	gi|197692221	150.4	39	15	3	28112	1.48	14-3-3 protein beta/alpha
Cell cycle and apoptosis process									
4308	LMNA	gi|21619981	96.91	25	11	11	53197	1.97	Prelamin-A/C
7601	KRT7	gi|67782365	167.69	50	28	19	51386	1.76	Keratin, type II cytoskeletal 7
8109	YWHAH	gi|119580405	138.95	26	12	1	26706	1.48	14-3-3 protein eta
8109	YWHAG	gi|5726310	138.17	25	11	1	28374	1.48	14-3-3 protein gamma
Metabolic process									
7104	CAPNS1	gi|51599151	142.77	34	8	1	28316	3.05	Calpain small subunit 1
7104	PDXK	gi|4505701	63.91	10	2	2	35102	3.05	Pyridoxal kinase
4308	MTHFD1	gi|30048109	101.93	37	14	14	32610	1.97	C-1-tetrahydrofolate synthase, cytoplasmic
4308	ACADVL	gi|119610652	55.51	6	4	4	72878	1.97	Very long-chain specific acyl-CoA dehydrogenase, mitochondrial
4308	NPM1	gi|13536991	47.25	9	3	3	28400	1.97	Nucleophosmin
3103	PGK1	gi|54673534	229.75	51	74	10	44615	1.74	Phosphoglycerate kinase 1
3103	ANXA2	gi|119597993	77.82	16	4	4	32449	1.74	Annexin A2
3103	TPI1	gi|15929332	132.69	60	16	16	26669	1.74	Triosephosphate isomerase 1
3103	PGK2	gi|31543397	165.85	26	27	3	44796	1.74	Phosphoglycerate kinase 2
4504	ENO1	gi|13325287	199.65	59	39	20	17788	1.47	Enolase 1
4504	ENO2	gi|930063	45.29	9	4	2	47154	1.47	Enolase 2
Protein folding									
3103	HSPA1A/1B	gi|4529893	111.46	32	13	10	41827	1.74	Heat shock 70 kDa protein 1A/1B
4104	GRPEL1	gi|119602776	83.69	37	7	7	19589	1.54	GrpE protein homolog 1, mitochondrial
4504	DNAJA2	gi|119603100	73.91	7	3	3	45746	1.47	DnaJ homolog subfamily A member 2
6102	TCP1	gi|119568001	146.67	20	11	11	60344	1.34	T-complex protein 1 subunit alpha

SSP no.	Gene symbol	Accession	-10lgP	Coverage (%)	#Peptides	#Unique	Avg. Mass	Log_2 fold change	Protein description
Proteolysis									
3103	PSMA6	gi|23110944	92.18	26	6	6	27399	1.74	Proteasome subunit alpha type-6
4104	PSMC3	gi|48145579	74.95	15	6	6	45250	1.54	26S protease regulatory subunit 6A
4104	PSMC1	gi|119601826	69.17	9	3	3	44507	1.54	26S protease regulatory subunit 4
6104	UCHL1	gi|119613387	216.23	67	34	1	24524	1.06	Ubiquitin carboxyl-terminal hydrolase isozyme L1
Structural molecule activity and cytoskeletal organisation									
7601	ACTG1	gi|4501887	208.49	79	54	2	41793	1.76	Actin, cytoplasmic 2
7601	ACTB	gi|13279023	197.83	79	42	1	41737	1.76	Actin, cytoplasmic 1
7601	KRT8	gi|90110027	101.64	20	11	6	53704	1.76	Keratin, type II cytoskeletal 8
4104	ARPC1A	gi|300360515	44.77	8	2	2	39659	1.54	Actin-related protein 2/3 complex subunit 1A
5506	KRT17	gi|119581157	187.82	73	41	12	48106	1.19	Keratin, type I cytoskeletal 17
5506	KRT19	gi|127796377	94.44	13	9	1	44092	1.19	Keratin, type I cytoskeletal 19
Transcriptional regulation									
4308	SRSF1	gi|21104372	109.07	31	9	9	27745	1.97	Serine/arginine-rich splicing factor 1
4308	SRSF7	gi|119620769	79.06	39	7	7	15257	1.97	Serine/arginine-rich splicing factor 7
3103	HMGB1	gi|13097234	73.36	13	5	5	24894	1.74	High mobility group protein B1
4504	FUS	gi|34481861	41.3	15	3	3	16107	1.47	RNA-binding protein FUS
7601	POTEF	gi|153791352	143.71	12	20	1	121444	1.76	POTE ankyrin domain family member F
Translational regulation									
7104	DDX47	gi|134254726	66.24	25	4	4	19802	3.05	ATP-dependent RNA helicase DDX47
3103	EEF2	gi|19353009	90.64	17	8	8	57500	1.74	Elongation factor 2
4504	PA2G4	gi|119617291	106.55	22	9	9	43787	1.47	Proliferation-associated 2G4
4504	EEF1G	gi|39644794	53.09	7	3	3	49845	1.47	Elongation factor 1-gamma
Transport									
7601	ACTA2	gi|178027	154.37	32	19	2	42108	1.76	Alpha actin
7601	ACTBL2	gi|63055057	131.04	25	14	3	42003	1.76	Beta-actin-like protein 2
4504	GDI2	gi|119606836	91.05	14	6	6	48312	1.47	Rab GDP dissociation inhibitor beta
4104	RAB7A	gi|20379060	73.46	30	6	6	23490	1.54	Ras-related protein Rab-7a

Note: [a] SSP number obtained from PDQuest software. [b] Gene symbol obtained from IPA analysis. [c] Accession number according to Homo sapiens protein database in NCBI (Aug 2013). [d] Proteins with -10lgP score >40 were selected for functional analysis. [e] Percentage of protein sequence covered by peptides detected in sample. [f] Number of peptides matched to protein sequence. [g] Number of peptides that are uniquely matched to protein sequence. [h] Average mass of protein.

Table 2
Functional classification of down-regulated proteins in CaSki cells treated with 3.5μM MS13.

SSP no.	Gene symbol	Accession	-10lgP	Coverage (%)	#Peptides	#Unique	Avg. Mass	Log_2 fold change	Protein description
Cell cycle									
8210	EMD	gi|119593149	44.32	10	2	2	24938	-1.76	Emerin
Immune system process									
8210	IL1A	gi|738207	45.43	7	1	1	18179	-1.76	Interleukin-1 alpha
Metabolic process									
1413	ALDOA	gi|28614	47.18	3	1	1	39332	-2.17	Fructose-bisphosphate aldolase A
8210	ATP5B	gi|179279	124.35	15	6	1	56896	-1.76	ATP synthase subunit beta, mitochondrial
8210	ANXA5	gi|809185	109.34	33	10	1	35937	-1.76	Annexin A5
Protein folding									
8902	HSP90B1	gi|15010550	223.78	43	45	42	90194	-2.61	Endoplasmin
8902	HSP90AB2P	gi|61104911	85.37	5	4	1	49123	-2.61	Heat shock protein 90kDa beta 2
Proteolysis									
6202	PSME2	gi|30410792	64.85	13	4	4	27402	-1.36	Proteasome activator complex subunit 2
Structural molecule activity									
8902	ACTN4	gi|2804273	53.08	1	1	1	102268	-2.61	Alpha-actinin-4
Transcriptional regulation									
1413	HNRNPL	gi|52632385	68.39	7	3	3	50561	-2.17	Heterogeneous nuclear ribonucleoprotein L
Unknown									
8902		gi|119597948	93.37	6	4	1	36267	-2.61	hCG1786469

Note: [a] SSP number obtained from PDQuest software. [b] Gene symbol obtained from IPA analysis. [c] Accession number according to Homo sapiens protein database in NCBI (Aug 2013). [d] Proteins with -10lgP score >40 were selected for functional analysis. [e] Percentage of protein sequence covered by peptides detected in sample. [f] Number of peptides matched to protein sequence. [g] Number of peptides that are uniquely matched to protein sequence. [h] Average mass of protein

DISCUSSION

In this study the highly up- and down-regulated DEPs associated with cell communication, metabolic process, cell cycle and apoptosis, transcriptional regulation, translational regulation, protein folding and structural molecule activity modulated by MS13 that could contribute to anticancer activity are discussed below. ARHGDIB negatively regulates GDP/GTP exchange reaction by preventing the dissociation of GDP from Rho proteins, thus limiting the conversion of inactive Rho proteins to active form.[16] The active GTP-bound form is associated with various cancer metastasis. ARHGDIB expression has been reported to be inversely correlated with the invasiveness of human bladder cancer cells[17] and it has been shown to suppress lung metastasis, inhibit cell invasion and reduce cell motility.[16] It may be inferred that upregulation of ARHGDIB by MS13 may suppress the metastatic properties of CaSki cells. Aberrant cell division is the hallmark of cancer cells. It is often associated with low expression of cell cycle-controlling proteins or overexpression of cell cycle-promoting proteins. LMNA is associated with cell cycle control and positively regulates pRB expression and protects it from proteasomal degradation. LMNA-knockout cells displayed an overall net effect of reduced capacity to undergo cell-cycle arrest in response to DNA damage due to the deregulation of pRB[18] suggesting that MS13 may initiate cell cycle arrest to suppress CaSki cell growth. Cancer cells generally alters cellular metabolism to support tumour proliferation.[19] Our data showed that highly upregulated proteins such as CAPNS1, PDXK, MTHFD1, ACADVL and NPM1 were associated with metabolic processes. CAPNS1 is a small regulatory subunit that stabilises the calcium-dependent cysteine proteinase, Calpain I and Calpain II, which catalyses the cleavage of proteins associated with cell adhesion, migration[20] and apoptosis.[21] 4-hydroxytamoxifen (4-OHT), often used to treat breast cancer, reportedly up-regulated CAPNS1 via induction of nuclear respiratory factor-1 which induced G1 phase cell cycle arrest.[22] Upregulation of CAPNS1 by MS13 may trigger cell cycle arrest in proliferating cells, thereby inhibiting cancer cell growth. PDXK catalyses the synthesis of pyridoxal-5'-phosphate, the biologically active form of vitamin B6. High PDXK level was correlated with good prognosis in patients with non-small cell lung cancer whilst cancer cells with vitamin B6-deficiency appeared to be more resistant to stress-induced death than their vitamin B6-proficient counterparts.[23] Therefore, modulation of vitamin B6 metabolism by MS13 may correlate with the induction of programmed cell death in treated cells. MTHFD1 is implicated in interconversion of one-carbon derivatives of bioactive folic acid, tetrahydrofolate. The activated one-carbon units are utilised in a wide range of cellular processes, such as *de novo* purine and thymidylate synthesis, serine and glycine interconversion, methionine biosynthesis, and protein synthesis. Similar to our findings, T-lymphoblastic leukaemia cells treated with doxorubicin and mitoxantrone also demonstrated up-regulation of MTHFD1.[24] ACADVL contributes to the generation of energy through catalysing the first step of mitochondrial fatty acid beta-oxidation. Treatment with curcumin and its analogue T63 induced upregulation of ACADVL, and demonstrated cell cycle arrest and apoptosis in lung cancer cells.[25] NPM1 is associated with diverse biological processes, such as ribosome biogenesis, chromatin remodelling[26], histone chaperone[27], centrosome duplication[28] and cell proliferation. Low NPM1 expression level was observed in gastric cancer and metastatic tissue samples compared to non-neoplastic and non-metastatic samples.[29] Upregulation of NPM1 was identified in HeLa cervical cancer cells following treatment with 6-Shagoal[30] and podophyllotoxin[31] and both treatments led to induction of apoptosis. Upregulation of these proteins in CaSki cells suggests that MS13 may modulate metabolic pathways and contributes to apoptosis and suppression of cell proliferation. Expression of transcription regulators, SRSF1 and SRSF7 were up-regulated in CaSki cells following MS13 treatment. SRSF1 and SRSF7 are implicated in constitutive and alternative splicing of pre-mRNAs.[32] The relationship between these proteins and tumorigenesis is not well-documented. However, elevated expression of SRSF1 was identified in response to colon cancer treatment using histone deacetylase inhibitor RC307 and cell growth inhibition was observed.[33] While there is insufficient information describing the roles of SRSF1 and SRSF7 in cancer development, upregulation of these proteins may facilitate anticancer role of MS13 via modulation of transcriptional regulation. Our proteomics data also indicated that DDX47, associated with translational regulation is one of the highly up-regulated proteins. The precise role of DDX47 is not fully understood. Several studies have demonstrated its involvement in ribosome biogenesis by mediating pre-rRNA processing[34] and initiation of apoptosis in cancer cells when interacted with $GABA_A$ receptor-associated protein.[35] While there is limited knowledge regarding the role of DDX47 in cancer progression, upregulation by MS13 may exhibit anticancer activity via induction of apoptosis. In the present study several highly down-regulated proteins were also noted in MS13 treated CaSki cells. MS13 treatment negatively regulated proteins associated with metabolic processes, such as ALDOA, ATP5B and ANXA5. ALDOA is a glycolytic enzyme that catalyses the reversible conversion of fructose-1,6-bisphosphate to glyceraldehyde-3-phosphate and dihydroxyacetone phosphate. Depletion of ALDOA has been proposed to decrease the growth of lung squamous cell carcinoma and reduced the risk of metastasis.[36] In fact, downregulation of ALDOA was also reported in neuroblastoma cells treated with curcumin, demonstrating inhibitory effects on cell growth.[37] Suppression of ALDOA by MS13 potentially decreases glucose metabolism that is required to support cell proliferation, thus mediating anti-proliferative activity in treated CaSki cells. ATP5B is a subunit of ATP synthase that generates ATP from ADP in the presence of a proton gradient across the membrane generated by the electron transport system.[38] ANXA5 was shown as an anticoagulant protein that inhibits the thromboplastin binding site, and interferes with the blood coagulation cascade.[39] It is also thought to function as an inhibitor of phospholipase A2, which is associated with phospholipid metabolism.[40] Prostate cancer cells treated with butylidenephthalide induced apoptosis and decreased cell viability by down-regulating ATP5B and

ANXA5.[41] Thus, suppression of these metabolic proteins may repress the activation of metabolic pathways that contributes to the anticancer properties of MS13. Heat shock proteins (HSPs) function as molecular chaperones assist in correct protein folding. They are highly expressed in cancer cells to facilitate tumour cell proliferation and survival. [42] Among these HSPs, we found that HSP90AB2P and HSP90B1 were downregulated in MS13-treated CaSki cells. To the best of our knowledge, there is no clearly defined data on the function of HSP90AB2P and its relationship to malignancy. Notably, treatment of lung cancer cells with curcumin and its analogue T63 showed downregulation of HSP90B1, which was responsible for the induction of apoptosis and cell cycle arrest.[25] Similarly, downregulation of HSPs in CaSki cells by MS13 may contribute to the anti-proliferative activity and induction of apoptosis. ACTN4, associated with structural molecule activity, is frequently correlated with increased cell motility, rapid cell division and cancer metastases.[43-45] In fact, curcumin-treated neuroblastoma cells [37] and berberine-treated breast cancer cells[46] demonstrated repression of ACTN4 and inhibition of cell growth in the treated cells. In a separate study, low ACTN4 expression was shown to decrease the invasiveness of pancreatic cancer cells.[47] This suggests that the downregulation of ACTN4 may be a strategy by which MS13 inhibits CaSki cell proliferation and reduce its invasiveness and metastatic potential. Transcriptional regulator HNRNPL is a multifunctional RNA-binding protein that plays a role as a repressor or activator of intron retention, exon skipping or inclusion, and alternative poly (A) site selection during alternative splicing.[48] Suppression of HNRNPL expression in non-small cell lung cancer lead to loss of tumorigenicity.[49] HNRNPL interacts with exonic splicing silencer, and increases the production of anti-apoptotic caspase-9b through exclusion of a 4-exon cassette, thus enhancing cancer cell survival. Downregulation of HNRNPL increases the production of pro-apoptotic caspase-9a through inclusion of the exons and promotes apoptosis of cancer cells.[49] This may reflect a similar mechanism by which MS13 downregulates HNRNPL and initiates apoptosis in CaSki cells.

CONCLUSION

Our study revealed that MS13 modulates key protein targets that may play important role in the anticancer mechanism of cervical cancer cells. These findings suggest that MS13 has therapeutic potential and may serve as chemotherapeutic agent for cervical cancer.

FUNDING ACKNOWLEDGEMENTS

We acknowledge the resources and financial support for the study was provided by the Fundamental Research Grant Scheme, (FRGS/1/2013/SKK01/MUSM/02/1) under the Ministry of Higher Education (MOHE), Malaysia. The generous support for carrying out the study at Jeffrey Cheah School of Medicine and Health Sciences, Monash University Malaysia, is also acknowledged.

CONFLICT OF INTEREST

Conflict of interest declared none.

REFERENCES

1. Ferlay J, Soerjomataram I, Dikshit R, Eser S, Mathers C, Rebelo M, et al. Cancer incidence and mortality worldwide: sources, methods and major patterns in GLOBOCAN 2012. Int J Cancer. 2015 [cited 2017 Mar 1];136(5):E359-86. Available from: http://www.ncbi.nlm.nih.gov/pubmed/25220842 DOI: 10.1002/ijc.29210
2. Adams AK, Wise-Draper TM, Wells SI. Human papillomavirus induced transformation in cervical and head and neck cancers. Cancers (Basel). 2014 [cited 2017 Mar 4];6(3):1793-820. Available from: http://www.ncbi.nlm.nih.gov/pubmed/25226287 DOI: 10.3390/cancers6031793
3. Peitsaro P, Johansson B, Syrjanen S. Integrated human papillomavirus type 16 is frequently found in cervical cancer precursors as demonstrated by a novel quantitative real-time PCR technique. J Clin Microbiol. 2002 [cited 2017 Mar 4];40(3):886-91. Available from: http://www.ncbi.nlm.nih.gov/pubmed/11880410 DOI:
4. Trimble CL, Piantadosi S, Gravitt P, Ronnett B, Pizer E, Elko A, et al. Spontaneous regression of high-grade cervical dysplasia: effects of human papillomavirus type and HLA phenotype. Clin Cancer Res. 2005 [cited 2017 Jul 01];11(13):4717-23. Available from: http://www.ncbi.nlm.nih.gov/pubmed/16000566 DOI: 10.1158/1078-0432.CCR-04-2599
5. Clifford GM, Smith JS, Plummer M, Munoz N, Franceschi S. Human papillomavirus types in invasive cervical cancer worldwide: a meta-analysis. Br J Cancer. 2003 [cited 2017 Jan 13];88(1):63-73. Available from: http://www.ncbi.nlm.nih.gov/pubmed/12556961 DOI: 10.1038/sj.bjc.6600688
6. Phillips JM, Clark C, Herman-Ferdinandez L, Moore-Medlin T, Rong X, Gill JR, et al. Curcumin inhibits skin squamous cell carcinoma tumor growth in vivo. Otolaryngol Head Neck Surg. 2011 [cited 2017 Jul 5];145(1):58-63. Available from: http://www.ncbi.nlm.nih.gov/pubmed/21493306 DOI: 10.1177/0194599811400711
7. Lu WD, Qin Y, Yang C, Li L, Fu ZX. Effect of curcumin on human colon cancer multidrug resistance in vitro and in vivo. Clinics (Sao Paulo). 2013 [cited 2017 May 23];68(5):694-701. Available from: http://www.ncbi.nlm.nih.gov/pubmed/23778405 DOI: 10.6061/clinics/2013(05)18
8. Divya CS, Pillai MR. Antitumor action of curcumin in human papillomavirus associated cells involves downregulation of viral oncogenes, prevention of NFkB and AP-1 translocation, and modulation of apoptosis. Mol Carcinog. 2006 [cited 2017 May 18];45(5):320-32. Available from:

http://www.ncbi.nlm.nih.gov/pubmed/16526022
DOI: 10.1002/mc.20170

9. Singh M, Singh N. Molecular mechanism of curcumin induced cytotoxicity in human cervical carcinoma cells. Mol Cell Biochem. 2009 [cited 2017 May 2];325(1-2):107-19. Available from: http://www.ncbi.nlm.nih.gov/pubmed/19191010 DOI: 10.1007/s11010-009-0025-5
10. Mukhopadhyay A, Banerjee S, Stafford LJ, Xia C, Liu M, Aggarwal BB. Curcumin-induced suppression of cell proliferation correlates with down-regulation of cyclin D1 expression and CDK4-mediated retinoblastoma protein phosphorylation. Oncogene. 2002 [cited 2016 Dec 12];21(57):8852-61. Available from: http://www.ncbi.nlm.nih.gov/pubmed/12483537 DOI: 10.1038/sj.onc.1206048
11. Prasad S, Tyagi AK, Aggarwal BB. Recent developments in delivery, bioavailability, absorption and metabolism of curcumin: the golden pigment from golden spice. Cancer Res Treat. 2014 [cited 2017 Jan 15];46(1):2-18. Available from: http://www.ncbi.nlm.nih.gov/pubmed/24520218 DOI: 10.4143/crt.2014.46.1.2
12. Paulraj F, Abas F, Lajis NH, Othman I, Hassan SS, Naidu R. The Curcumin Analogue 1,5-Bis(2-hydroxyphenyl)-1,4-pentadiene-3-one Induces Apoptosis and Downregulates E6 and E7 Oncogene Expression in HPV16 and HPV18-Infected Cervical Cancer Cells. Molecules. 2015 [cited 2017 April 26];20(7):11830-60. Available from: http://www.ncbi.nlm.nih.gov/pubmed/26132907 DOI: 10.3390/molecules200711830
13. Friedman L, Lin L, Ball S, Bekaii-Saab T, Fuchs J, Li PK, et al. Curcumin analogues exhibit enhanced growth suppressive activity in human pancreatic cancer cells. Anticancer Drugs. 2009 [cited 2017 Jul 1];20(6):444-9. Available from: http://www.ncbi.nlm.nih.gov/pubmed/19384191 DOI: 10.1097/CAD.0b013e32832afc04
14. Lin L, Hutzen B, Ball S, Foust E, Sobo M, Deangelis S, et al. New curcumin analogues exhibit enhanced growth-suppressive activity and inhibit AKT and signal transducer and activator of transcription 3 phosphorylation in breast and prostate cancer cells. Cancer Sci. 2009 [cited 2016 Sep 10];100(9):1719-27. Available from: http://www.ncbi.nlm.nih.gov/pubmed/19558577 DOI: 10.1111/j.1349-7006.2009.01220.x
15. Lee KH, Ab Aziz FH, Syahida A, Abas F, Shaari K, Israf DA, et al. Synthesis and biological evaluation of curcumin-like diarylpentanoid analogues for anti-inflammatory, antioxidant and anti-tyrosinase activities. Eur J Med Chem. 2009 [cited 2016 Aug 30];44(8):3195-200. Available from: http://www.ncbi.nlm.nih.gov/pubmed/19359068 DOI: 10.1016/j.ejmech.2009.03.020
16. Gildea JJ, Seraj MJ, Oxford G, Harding MA, Hampton GM, Moskaluk CA, et al. RhoGDI2 is an invasion and metastasis suppressor gene in human cancer. Cancer Res. 2002 [cited 2016 Nov 15];62(22):6418-23. Available from: http://www.ncbi.nlm.nih.gov/pubmed/12438227 DOI:
17. Seraj MJ, Harding MA, Gildea JJ, Welch DR, Theodorescu D. The relationship of BRMS1 and RhoGDI2 gene expression to metastatic potential in lineage related human bladder cancer cell lines. Clin Exp Metastasis. 2000 [cited 2017 Feb 12];18(6):519-25. Available from: http://www.ncbi.nlm.nih.gov/pubmed/11592309 DOI:
18. Johnson BR, Nitta RT, Frock RL, Mounkes L, Barbie DA, Stewart CL, et al. A-type lamins regulate retinoblastoma protein function by promoting subnuclear localization and preventing proteasomal degradation. Proc Natl Acad Sci U S A. 2004 [cited 2016 Jun 29];101(26):9677-82. Available from: http://www.ncbi.nlm.nih.gov/pubmed/15210943 DOI: 10.1073/pnas.0403250101
19. Locasale JW, Cantley LC. Altered metabolism in cancer. BMC Biol. 2010 [cited 2017 Jan 10];8:88. Available from: http://www.ncbi.nlm.nih.gov/pubmed/20598111 DOI: 10.1186/1741-7007-8-88
20. Undyala VV, Dembo M, Cembrola K, Perrin BJ, Huttenlocher A, Elce JS, et al. The calpain small subunit regulates cell-substrate mechanical interactions during fibroblast migration. J Cell Sci. 2008 [cited 2016 Nov 1];121(Pt 21):3581-8. Available from: http://www.ncbi.nlm.nih.gov/pubmed/18840650 DOI: 10.1242/jcs.036152
21. Tan Y, Wu C, De Veyra T, Greer PA. Ubiquitous calpains promote both apoptosis and survival signals in response to different cell death stimuli. J Biol Chem. 2006 [cited 2016 Jun 30];281(26):17689-98. Available from: http://www.ncbi.nlm.nih.gov/pubmed/16632474 DOI: 10.1074/jbc.M601978200
22. Ivanova MM, Luken KH, Zimmer AS, Lenzo FL, Smith RJ, Arteel MW, et al. Tamoxifen increases nuclear respiratory factor 1 transcription by activating estrogen receptor beta and AP-1 recruitment to adjacent promoter binding sites. FASEB J. 2011 [cited 2017 Apr 27];25(4):1402-16. Available from: http://www.ncbi.nlm.nih.gov/pubmed/21233487 DOI: 10.1096/fj.10-169029
23. Galluzzi L, Vitale I, Senovilla L, Olaussen KA, Pinna G, Eisenberg T, et al. Prognostic impact of vitamin B6 metabolism in lung cancer. Cell Rep. 2012 [cited 2016 Aug 30];2(2):257-69. Available from: http://www.ncbi.nlm.nih.gov/pubmed/22854025 DOI: 10.1016/j.celrep.2012.06.017
24. Tyleckova J, Hrabakova R, Mairychova K, Halada P, Radova L, Dzubak P, et al. Cancer cell response to anthracyclines effects: mysteries of the hidden proteins associated with these drugs. Int J Mol Sci. 2012 [cited 2017 Feb 28];13(12):15536-64. Available from: http://www.ncbi.nlm.nih.gov/pubmed/23443080 DOI: 10.3390/ijms131215536
25. Liu H, Liu YZ, Zhang F, Wang HS, Zhang G, Zhou BH, et al. Identification of potential pathways involved in the induction of cell cycle arrest and

apoptosis by a new 4-arylidene curcumin analogue T63 in lung cancer cells: a comparative proteomic analysis. Mol Biosyst. 2014 [cited 2016 Jun 18];10(6):1320-31. Available from: http://www.ncbi.nlm.nih.gov/pubmed/24651282 DOI: 10.1039/c3mb70553f

26. Lindstrom MS. NPM1/B23: A Multifunctional Chaperone in Ribosome Biogenesis and Chromatin Remodeling. Biochem Res Int. 2011 [cited 2017 Mar 5];2011:195209. Available from: http://www.ncbi.nlm.nih.gov/pubmed/21152184 DOI: 10.1155/2011/195209
27. Gadad SS, Senapati P, Syed SH, Rajan RE, Shandilya J, Swaminathan V, et al. The multifunctional protein nucleophosmin (NPM1) is a human linker histone H1 chaperone. Biochemistry. 2011 [cited 2017 Apr 12];50(14):2780-9. Available from: http://www.ncbi.nlm.nih.gov/pubmed/21425800 DOI: 10.1021/bi101835j
28. Okuda M. The role of nucleophosmin in centrosome duplication. Oncogene. 2002 [cited 2016 Sep 9];21(40):6170-4. Available from: http://www.ncbi.nlm.nih.gov/pubmed/12214246 DOI: 10.1038/sj.onc.1205708
29. Leal MF, Mazzotti TK, Calcagno DQ, Cirilo PD, Martinez MC, Demachki S, et al. Deregulated expression of Nucleophosmin 1 in gastric cancer and its clinicopathological implications. BMC Gastroenterol. 2014 [cited 2017 Apr 12];14:9. Available from: http://www.ncbi.nlm.nih.gov/pubmed/24410879 DOI: 10.1186/1471-230X-14-9
30. Liu Q, Peng YB, Qi LW, Cheng XL, Xu XJ, Liu LL, et al. The Cytotoxicity Mechanism of 6-Shogaol-Treated HeLa Human Cervical Cancer Cells Revealed by Label-Free Shotgun Proteomics and Bioinformatics Analysis. Evid Based Complement Alternat Med. 2012 [cited 2017 April 24];2012:278652. Available from: http://www.ncbi.nlm.nih.gov/pubmed/23243437 DOI: 10.1155/2012/278652
31. Wang B, Chen L, Zhen H, Zhou L, Shi P, Huang Z. Proteomic changes induced by podophyllotoxin in human cervical carcinoma HeLa cells. Am J Chin Med. 2013 [cited 2017 Apr 27];41(1):163-75. Available from: http://www.ncbi.nlm.nih.gov/pubmed/23336514 DOI: 10.1142/S0192415X13500122
32. Haynes C, Iakoucheva LM. Serine/arginine-rich splicing factors belong to a class of intrinsically disordered proteins. Nucleic Acids Res. 2006 [cited 2017 Mar 16];34(1):305-12. Available from: http://www.ncbi.nlm.nih.gov/pubmed/16407336 DOI: 10.1093/nar/gkj424
33. Milli A, Cecconi D, Campostrini N, Timperio AM, Zolla L, Righetti SC, et al. A proteomic approach for evaluating the cell response to a novel histone deacetylase inhibitor in colon cancer cells. Biochim Biophys Acta. 2008 [cited 2016 Nov 6];1784(11):1702-10. Available from: http://www.ncbi.nlm.nih.gov/pubmed/18503786 DOI: 10.1016/j.bbapap.2008.04.022
34. Tafforeau L, Zorbas C, Langhendries JL, Mullineux ST, Stamatopoulou V, Mullier R, et al. The complexity of human ribosome biogenesis revealed by systematic nucleolar screening of Pre-rRNA processing factors. Mol Cell. 2013 [cited 2016 Aug 22];51(4):539-51. Available from: http://www.ncbi.nlm.nih.gov/pubmed/23973377 DOI: 10.1016/j.molcel.2013.08.011
35. Lee JH, Rho SB, Chun T. GABAA receptor-associated protein (GABARAP) induces apoptosis by interacting with DEAD (Asp-Glu-Ala-Asp/His) box polypeptide 47 (DDX 47). Biotechnol Lett. 2005 [cited 2017 May 2];27(9):623-8. Available from: http://www.ncbi.nlm.nih.gov/pubmed/15977068 DOI: 10.1007/s10529-005-3628-2
36. Du S, Guan Z, Hao L, Song Y, Wang L, Gong L, et al. Fructose-bisphosphate aldolase a is a potential metastasis-associated marker of lung squamous cell carcinoma and promotes lung cell tumorigenesis and migration. PLoS One. 2014 [cited 2017 Feb 5];9(1):e85804. Available from: http://www.ncbi.nlm.nih.gov/pubmed/24465716 DOI: 10.1371/journal.pone.0085804
37. D'Aguanno S, D'Agnano I, De Canio M, Rossi C, Bernardini S, Federici G, et al. Shotgun proteomics and network analysis of neuroblastoma cell lines treated with curcumin. Mol Biosyst. 2012 [cited 2017 Apr 11];8(4):1068-77. Available from: http://www.ncbi.nlm.nih.gov/pubmed/22315092 DOI: 10.1039/c2mb05498a
38. Jonckheere AI, Smeitink JA, Rodenburg RJ. Mitochondrial ATP synthase: architecture, function and pathology. J Inherit Metab Dis. 2012 [cited 2017 Mar 8];35(2):211-25. Available from: http://www.ncbi.nlm.nih.gov/pubmed/21874297 DOI: 10.1007/s10545-011-9382-9
39. Andree HA, Stuart MC, Hermens WT, Reutelingsperger CP, Hemker HC, Frederik PM, et al. Clustering of lipid-bound annexin V may explain its anticoagulant effect. J Biol Chem 1992;267(25):17907-12.
40. Buckland AG, Wilton DC. Inhibition of secreted phospholipases A2 by annexin V. Competition for anionic phospholipid interfaces allows an assessment of the relative interfacial affinities of secreted phospholipases A2. Biochim Biophys Acta 1998;1391(3):367-76.
41. Pang CY, Chiu SC, Harn HJ, Zhai WJ, Lin SZ, Yang HH. Proteomic-based identification of multiple pathways underlying n-butylidenephthalide-induced apoptosis in LNCaP human prostate cancer cells. Food Chem Toxicol. 2013 [cited 2016 Sep 17];59:281-8. Available from: http://www.ncbi.nlm.nih.gov/pubmed/23770345 DOI: 10.1016/j.fct.2013.05.045
42. Ciocca DR, Calderwood SK. Heat shock proteins in cancer: diagnostic, prognostic, predictive, and treatment implications. Cell Stress Chaperones 2005;10(2):86-103.
43. Khurana S, Chakraborty S, Cheng X, Su YT, Kao HY. The actin-binding protein, actinin alpha 4 (ACTN4), is a nuclear receptor coactivator that promotes proliferation of MCF-7 breast cancer cells. J Biol Chem. 2011 [cited 2017 Jan 21];286(3):1850-9. Available from:

http://www.ncbi.nlm.nih.gov/pubmed/21078666
DOI: 10.1074/jbc.M110.162107

44. Honda K, Yamada T, Hayashida Y, Idogawa M, Sato S, Hasegawa F, et al. Actinin-4 increases cell motility and promotes lymph node metastasis of colorectal cancer. Gastroenterology. 2005 [cited 2017 Jan 27];128(1):51-62. Available from: http://www.ncbi.nlm.nih.gov/pubmed/15633123
DOI:
45. Quick Q, Skalli O. Alpha-actinin 1 and alpha-actinin 4: contrasting roles in the survival, motility, and RhoA signaling of astrocytoma cells. Exp Cell Res. 2010 [cited 2017 Apr 15];316(7):1137-47. Available from: http://www.ncbi.nlm.nih.gov/pubmed/20156433
DOI: 10.1016/j.yexcr.2010.02.011
46. Chou HC, Lu YC, Cheng CS, Chen YW, Lyu PC, Lin CW, et al. Proteomic and redox-proteomic analysis of berberine-induced cytotoxicity in breast cancer cells. J Proteomics. 2012 [cited 2016 Jun 18];75(11):3158-76. Available from: http://www.ncbi.nlm.nih.gov/pubmed/22522123
DOI: 10.1016/j.jprot.2012.03.010
47. Hayashida Y, Honda K, Idogawa M, Ino Y, Ono M, Tsuchida A, et al. E-cadherin regulates the association between beta-catenin and actinin-4. Cancer Res. 2005 [cited 2016 Oct 1];65(19):8836-45. Available from: http://www.ncbi.nlm.nih.gov/pubmed/16204054
DOI: 10.1158/0008-5472.CAN-05-0718
48. Hung LH, Heiner M, Hui J, Schreiner S, Benes V, Bindereif A. Diverse roles of hnRNP L in mammalian mRNA processing: a combined microarray and RNAi analysis. RNA. 2008 [cited 2017 Feb 2];14(2):284-96. Available from: http://www.ncbi.nlm.nih.gov/pubmed/18073345
DOI: 10.1261/rna.725208
49. Goehe RW, Shultz JC, Murudkar C, Usanovic S, Lamour NF, Massey DH, et al. hnRNP L regulates the tumorigenic capacity of lung cancer xenografts in mice via caspase-9 pre-mRNA processing. J Clin Invest. 2010 [cited 2016 Nov 11];120(11):3923-39. Available from: http://www.ncbi.nlm.nih.gov/pubmed/20972334
DOI: 10.1172/JCI43552.

Reviewers of this article

Dr Shar Mariam Bt Mohamed

Associate Professor, International Medical University, No 126, Jalan Jalil Perkasa 19, Bukit Jalil, Kuala Lumpur

Asst. Prof. Dr. Deepansh Sharma, M.Sc, M.Phil, Ph.D.

Assistant Professor, School of Biotechnology and Bioscience, Lovely Professional University, Phagwara, Punjab, India

Prof.Dr.K.Suriaprabha

Asst. Editor , International Journal of Pharma and Bio sciences.

Prof.P.Muthuprasanna

Managing Editor , International Journal of Pharma and Bio sciences.

We sincerely thank the above reviewers for peer reviewing the manuscript